

Dramatic enhancement of 1.54 μm emission in Er doped GaN quantum well structures

T. M. Al tahtamouni,¹ M. Stachowicz,² J. Li,³ J. Y. Lin,³ and H. X. Jiang³

¹Department of Physics, Yarmouk University, Irbid 21163, Jordan

²Institute of Physics, Polish Academy of Sciences, 02-668 Warsaw, Poland

³Department of Electrical and Computer Engineering, Texas Tech University, Lubbock, Texas 79409, USA

(Received 9 January 2015; accepted 17 March 2015; published online 24 March 2015)

Erbium (Er) doped III-nitride materials have attracted much attention due to their capability to provide highly thermal stable optical emission in the technologically important as well as eye-safer 1540 nm wavelength window. There is a continued need to exploring effective mechanisms to further improve the quantum efficiency (QE) of the 1.54 μm emission in Er-doped III-nitrides. GaN/AlN multiple quantum wells (MQWs:Er) have been synthesized by metal organic chemical vapor deposition and explored as an effective means to improve the QE of the 1.54 μm emission via carrier confinement and strain engineering. The 1.54 μm emission properties from MQWs:Er were probed by photoluminescence (PL) emission spectroscopy. It was found that the emission intensity from MQWs:Er is 9 times higher than that of GaN:Er epilayers with a comparable Er active layer thickness. The influences of the well and barrier width on the PL emission at 1.54 μm were studied. The results revealed that MQWs:Er consisting of well width between 1 and 1.5 nm and the largest possible barrier width before reaching the critical thickness provide the largest boost in QE of the 1.54 μm emission. These results demonstrate that MQWs:Er provide a basis for efficient photonic devices active at 1.54 μm . © 2015 AIP Publishing LLC. [<http://dx.doi.org/10.1063/1.4916393>]

The intra-4f shell transitions of rare earth (RE) ions doped in a solid host give rise to sharp emission lines whose wavelengths are independent of host materials, since the wavefunctions of the 4f-electrons are highly confined in space and are very well screened by the outer closed 5s² and 5p⁶ shells.¹ Much of the research work on RE doping into semiconductors has focused on the element erbium for potential applications in optical communications. Doped in a solid material, erbium ion (Er³⁺) has an allowable intra 4f shell transition from its first excited state (⁴I_{13/2}) to the ground state (⁴I_{15/2}), leading to 1.54 μm emission which falls within the minimum loss window of silica fibers used in optical communications.^{2–8} Furthermore, the maximum permissible laser exposure limits at 1.54 μm for the eye-safety are several orders of magnitude higher than wavelengths near or below the neodymium emission line at 1.06 μm . Thus, solid-state lasers emitting at 1.54 μm based on Er doped materials are eye-safer and preferred in many applications where laser beams must be transmitted through the open air. Although the wavelength of emission is not affected by the solid host, the transition probability (i.e., emission intensity) is affected by the neighboring environment. It has been observed that the 1.54 μm emission from Er doped semiconductors of smaller bandgaps has a low efficiency at room temperature due to a strong thermal quenching effect.^{9,10} In general, the thermal stability of Er emission increases with an increase of the energy gap and *ionicity* of the host materials.^{9–12} Therefore, III-nitride semiconductors are excellent host materials for Er ions due to their wide bandgaps as well as their structural and thermal stabilities. Among III-nitrides, GaN is the most widely studied and has proven to be an outstanding host for Er, with reports of fabrication of light-emitting diodes operating in the visible and infrared region.¹³

However, further improvements in the quantum efficiency (QE) of the 1.54 μm emission in Er-doped III-nitrides are still needed to enable practical photonic devices.

Er³⁺ ions can be excited through electron-hole pair mediated processes in Er doped GaN through an above bandgap or near band-edge excitation.¹³ One way to improve the quantum efficiency of these device structures is to improve the excitation efficiency of the Er ions via the enhancement in the carrier density around Er³⁺ ions. This could be achieved by implementing quantum well (QW) structures.¹⁴ Doping Er into the well layers confined by the barriers is expected to improve the Er ions excitation efficiency under an above bandgap or near band-edge excitation. The QW architecture enhances both the spatial confinement and density of states of carriers within the well layers leading to an increase in the carrier density and energy transfer from carriers to Er³⁺ ions. Furthermore, the use of the QW architecture allows the flexibility in strain engineering which was shown to be an effective means in optimizing the emission characteristics of Er doped semiconductors.^{15,16}

In this work, Er-doped GaN/AlN multiple QWs (MQWs:Er) were synthesized by metal-organic chemical vapor deposition (MOCVD). The effects of the well and the barrier thicknesses of the MQW:Er on the emission intensity at 1.54 μm have been investigated. The 1.54 μm emission intensity was found to increase with increasing the barrier width. It was also demonstrated that the MQW architecture enhances the 1.54 μm emission intensity by a factor of 9 over the GaN:Er epilayers with a comparable Er doped active layer thickness. The largest enhancement was obtained in MQWs:Er with a well width between 1.0 and 1.5 nm.

MQWs:Er were grown on c-plane sapphire substrates using MOCVD. The aluminum source was trimethylaluminum

(TMA), the gallium source was trimethylgallium (TMGa), and the nitrogen source was ammonia (NH_3). Trisopropyl cyclopentadienylerbium (TRIPeR) was used as the *in-situ* Er doping source. Hydrogen was the carrier gas and was kept constant at 2 standard liters per minute (SLM). The growth started with a thin (30 nm) AlN buffer layer (buffer 1) grown at 950°C and 30 mbars followed by a second 100 nm AlN buffer layer (buffer 2) at 1100°C grown at 30 mbars, and a $1.0\ \mu\text{m}$ AlN template grown at 1300°C and 30 mbars.¹⁷ It was then followed by the growth of the MQWs:Er structure consisting of alternating layers of Er doped GaN wells and undoped AlN barriers. The growth temperature and pressure were 1020°C and 30 mbars, respectively. Figure 1 shows the layer structure of MQWs:Er samples. All samples were grown at the same Er molar flow rate. The well and barrier widths were determined by the pre-calibrated growth rates of the Er-doped GaN and undoped AlN epilayers, as determined by the *in-situ* spectroscopic reflectance. X-ray diffraction (XRD) was used to analyze the structures of MQWs:Er. Photoluminescence (PL) spectroscopy was employed to probe the well and barrier widths dependence of the Er related emission at $1.54\ \mu\text{m}$. PL measurements were carried out at room temperature (300 K) using a diode laser with an excitation wavelength (λ_{exc}) at 375 nm, providing a near band-edge excitation. An InGaAs detector was used to measure the emission spectra in the $1.54\ \mu\text{m}$ spectral window. Two different Er doped GaN/AlN MQW structures were investigated. The first set of MQW samples has a fixed

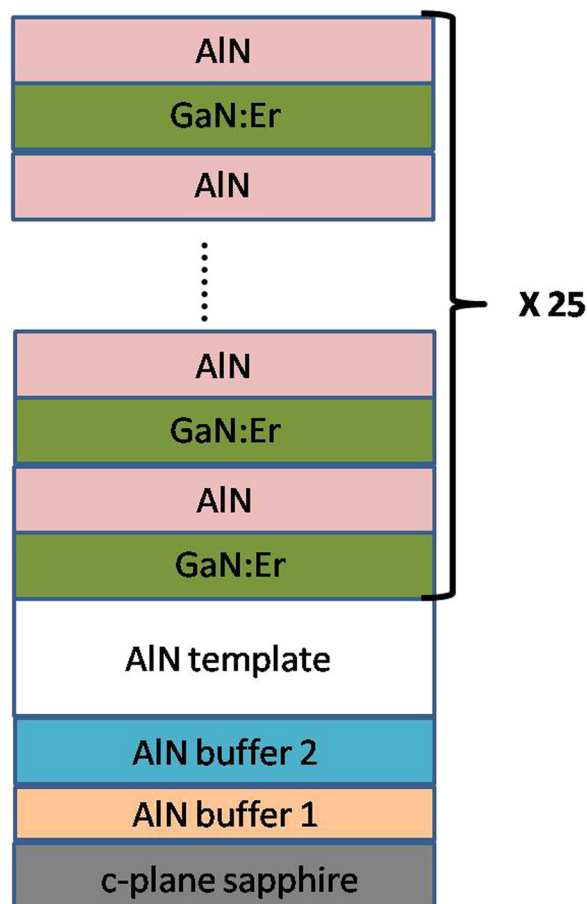


FIG. 1. Schematic layer structure of Er doped GaN/AlN multiple quantum wells (MQWs:Er) grown on AlN/sapphire template.

barrier thickness of 10 nm and a varying well width from 0.6, 1, 1.5, 2.8, 4, 5.3 to 6.6 nm. The second set of samples has a fixed well width of 1.5 nm and a varying barrier width from 3, 5, 7 to 10 nm.

X-ray θ - 2θ measurements for the Er doped GaN/AlN MQWs were performed to evaluate the structural characteristics of the MQWs:Er. Figure 2 shows the X-ray θ - 2θ scans of a set of MQWs:Er samples consisting of 25 periods of alternating Er doped GaN wells with various well widths $L_W = 0.6, 1, 1.5, 2.8, 4, 5.3,$ and 6.6 nm and AlN barrier with a fixed width $L_B = 10$ nm. The peaks at $2\theta = 36.0^\circ$ in Fig. 2 originate from the (0002) plane of the undoped AlN template, and the satellite peaks come from the Er doped GaN/AlN MQWs. The well-defined satellite peaks in X-ray diffraction spectra of all samples indicate that the interfaces between the wells and barriers are quite abrupt.¹⁸ As shown in Fig. 2, MQW:Er samples with thinner wells have large numbers of intense satellite peaks, indicating that these samples possess higher interfacial qualities than those with thicker wells. This can be attributed to the deterioration of the interfacial structural quality of the MQWs:Er caused by the generation of defects at the interface as the well width approaching the critical thickness of MQWs.¹⁹ The period Λ of a quantum well can be calculated by using the following equation:²⁰

$$\Lambda = (L_j - L_i)\lambda / 2(\sin \theta_j - \sin \theta_i), \quad (1)$$

where λ is the wavelength of the incident X-ray, L_j and L_i are diffraction orders of the QWs, θ_j and θ_i are the

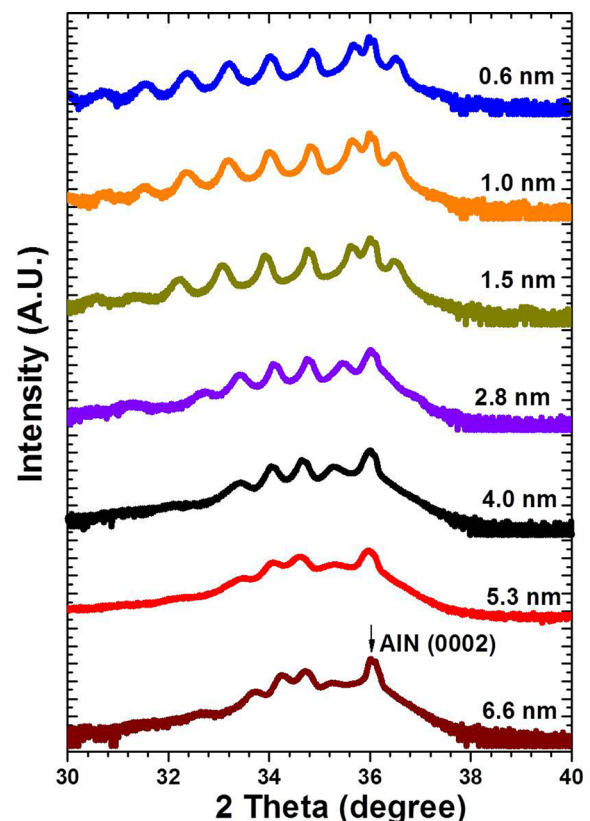


FIG. 2. X-ray theta-2theta diffraction measurement results of Er doped GaN/AlN MQWs with different GaN:Er well widths ($L_W = 0.6, 1, 1.5, 2.8, 4, 5.3,$ and 6.6 nm) and fixed AlN barrier width ($L_B = 10$ nm).

corresponding diffraction angles of those diffraction orders. As the period of MQW increases, the intervals between the satellite peaks are getting smaller. The XRD results are consistent with the targeted well and barrier widths based on the growth rates of the Er-doped GaN and undoped AlN epilayers.

Figure 3 compares the room temperature PL spectra between a 25 period MQWs:Er sample with a well/barrier width of $L_W = 1.5 \text{ nm}/L_B = 10 \text{ nm}$ and a GaN:Er epilayer of 38 nm in thickness. Both samples have a similar Er doped active layer thickness and were grown on the same AlN template with the same Er molar flow rate. Both samples exhibit emission peak at $1.54 \mu\text{m}$, corresponding to the intra- $4f$ Er^{3+} transitions from the first excited state (${}^4I_{13/2}$) to the ground state (${}^4I_{15/2}$). It is quite remarkable that the intensity of the $1.54 \mu\text{m}$ emission peak from MQWs:Er is 9 times higher than that from GaN:Er epilayer with a comparable Er active layer thickness. This large enhancement indicates that the MQW architecture significantly enhances the excitation efficiency of Er^{3+} owing to the enhanced carrier density in quantum wells. The full width at half maximum (FWHM) of the $1.54 \mu\text{m}$ emission peak is 60 and 50 nm for MQWs:Er and GaN:Er, respectively. The broadening of the emission peak in MQWs is due to thickness fluctuations of the wells and different atomic configuration around Er-centers. Er ions located in close proximity to the interfaces feel alloy-like AlGaIn environment and their emission contributes to inhomogeneous broadening of the spectral lines. In the case of a 1.5 nm well (3 unit cells), a large number of Er^{3+} ions in the well are located close to interfaces. The high growth temperature may also cause penetration of Er ions into barriers thus increasing inhomogeneous spectral lines broadening.

The room temperature (300 K) PL spectra of the $1.54 \mu\text{m}$ emission of the first set of MQWs:Er samples having 25 periods, fixed barrier width (10 nm), and varying well widths of 0.6, 1.0, 1.5, 2.8, 4.0, 5.3, and 6.6 nm are presented in Fig. 4(a). It can be seen that the $1.54 \mu\text{m}$ emission spectral line shape is independent of the well width. However, the

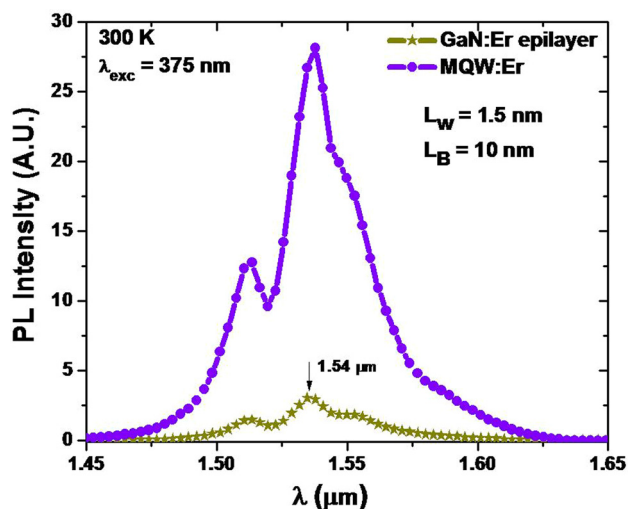


FIG. 3. Comparison of room temperature (300 K) of PL spectra of Er related emission near $1.54 \mu\text{m}$ between an Er doped GaN/AlN MQWs sample (having 25 periods and a well/barrier width of $L_W = 1.5 \text{ nm}/L_B = 10 \text{ nm}$) and Er doped GaN epilayer of 38 nm in thickness.

emission efficiency strongly depends on the well width. The well width dependence of the integrated PL intensity of the $1.54 \mu\text{m}$ emission for this set of MQWs:Er samples can be obtained from Fig. 4(a). Figure 4(b) shows the normalized $1.54 \mu\text{m}$ emission intensity (emission intensity normalized to the total thickness of the Er active layers in the MQWs:Er) versus the well width measured at 300 K for this set of MQWs:Er samples with a fixed barrier width of 10 nm. The horizontal dashed line represents the normalized $1.54 \mu\text{m}$ emission intensity of the GaN:Er epilayer of 38 nm in thickness, which is set to unity for comparison. The largest enhancement in PL intensity is achieved when the well width is in between 1 and 1.5 nm. The increase of the PL intensity per active layer thickness in MQWs:Er with decreasing the well thickness can be attributed partly to the enhanced carrier density around the Er ions in the active well regions due to quantum confinement, yielding an improved excitation efficiency of Er ions. Furthermore, GaN/AlN MQWs are highly strained due to the lattice mismatch of more than 2% between GaN and AlN, which induces an internal built-in electric field on the order of 4 MV/cm.²¹ The electric field acting upon charge carriers leads to their spatial separation and thus restrict formation of excitons which are necessary for excitation of the $4f$ -shell of Er^{3+} ions.¹⁴ It is well known

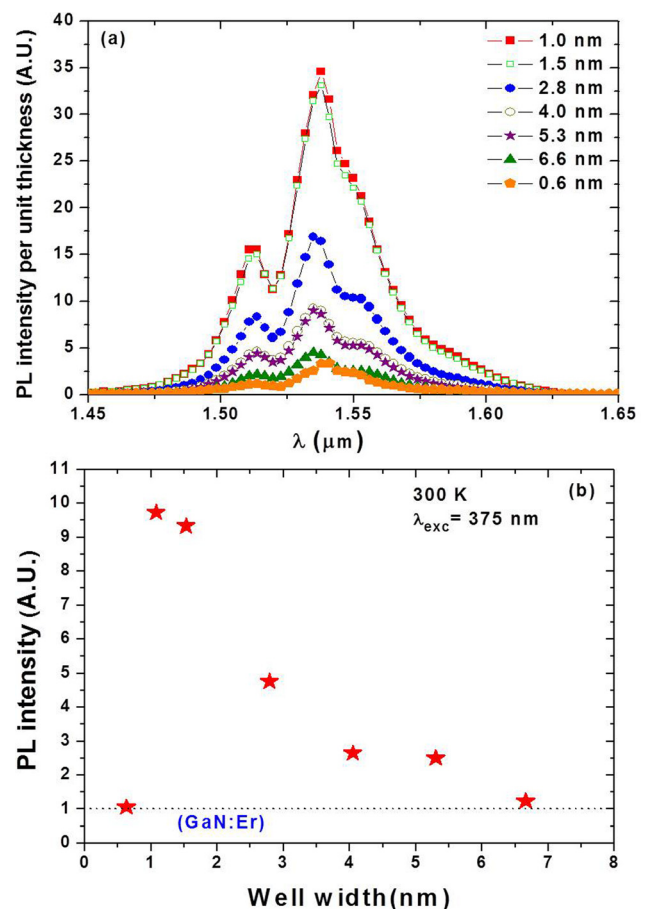


FIG. 4. (a) Room temperature (300 K) PL spectra near $1.54 \mu\text{m}$ of MQWs:Er with different well widths ($L_W = 0.6, 1, 1.5, 2.8, 4, 5.3,$ and 6.6 nm) and fixed AlN barrier width ($L_B = 10 \text{ nm}$). (b) The normalized PL intensity at $1.54 \mu\text{m}$ as a function of the well width. The horizontal dashed line represents the normalized $1.54 \mu\text{m}$ emission intensity of the GaN:Er epilayer of 38 nm in thickness, which is set to unity for comparison.

that built-in electric fields are detrimental for recombination efficiency in polar GaN/AlGaIn quantum structures, particularly for wells thickness higher than free exciton Bohr radius. Therefore, reduction of the Er emission efficiency will be stronger in wide GaN QWs, in agreement with the experimental data in Fig. 4. In Ref. 22, it was shown that in polar GaN/AlN MQW heterostructures the GaN well thickness already of 1.8 nm reduces the band gap of the well below that for bulk GaN,²³ so the wavelength of 375 nm (3.31 eV) is sufficient for over the band gap excitation. As a result, the excitation efficiency of Er³⁺ ions in 5 and 6 nm wells is much more reduced than it could be estimated from the intensity ratio of the PL spectra for 1.5 and 6 nm wells. Also, there was no absorption of 375 nm photons by AlN barriers. On the other hand, one can notice the decreased 1.54 μm emission intensity in MQWs:Er with well width smaller than 1 nm, which can be due to the enhanced carrier (or carrier wavefunctions) leakage into the barrier regions,^{14,19,21} which effectively reduces the carrier density in the Er doped active QW regions. This structure should be rather considered as a quasi-ternary alloy with periodically doped areas than as a MQW structure. Taking into account thickness fluctuations in GaN/AlN superlattices, typically within 0.4–0.6 nm,²² it is not clear whether for a 0.6 nm width (one unit cell) the quantum well is formed. If not, charge carriers remain delocalized.

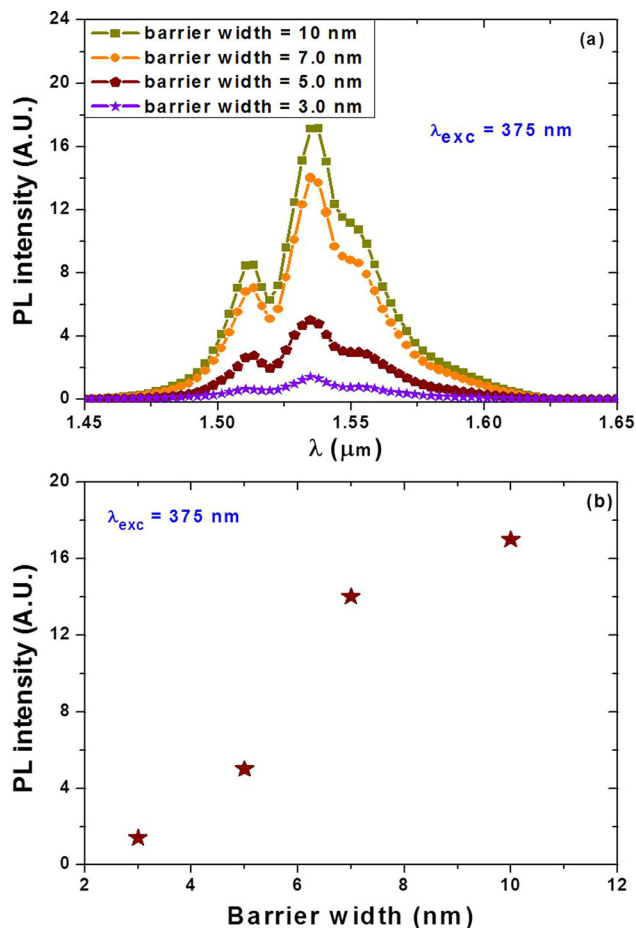


FIG. 5. (a) Room temperature (300K) PL spectra near 1.54 μm of MQWs:Er with different AlN barrier widths ($L_B = 3, 5, 7,$ and 10 nm) and fixed GaN:Er well width ($L_W = 1.5$ nm). (b) The PL intensity at 1.54 μm as a function of the barrier width.

Figure 5(a) shows the 300 K PL spectra in the 1.54 μm region obtained from MQWs:Er samples having 30 periods of GaN:Er wells and AlN barriers, a fixed well width (1.5 nm), and varying AlN barrier thicknesses (3.0, 5.0, 7.0, and 10 nm). It can be seen that the 1.54 μm emission line shape is independent of the barrier width. However, the PL intensity increases almost linearly with an increase in the barrier width as illustrated in Fig. 5(b). By changing the barrier width from 3.0 to 10 nm, the intensity of the 1.54 μm emission is enhanced by a factor of almost 12. The exciton Bohr radius in GaN is estimated to be 28 Å,²⁴ therefore, the electron wavefunctions can easily penetrate through the barrier layers and became delocalized. Interwell coupling will reduce the probability of capturing of excitons by Er-centers consequently leading to low excitation efficiency of Er³⁺ ions. Another explanation is related to strain in MQW structures. Previous studies carried out on GaN:Er¹⁵ and Si:Er + O and Si_xGe_{1-x}:Er + O materials¹⁶ have shown that the 1.54 μm emission intensity increases linearly with the magnitude of tensile or compressive stress. For GaN/AlN MQWs:Er, it is expected that the stress in the MQW structure and hence the emission intensity at 1.54 μm increase with increase of the barrier width.

In summary, GaN/AlN MQWs architecture was proposed as an effective means for dramatically enhancing the quantum efficiency of the 1.54 μm emission in Er doped GaN via quantum confinement. Er doped GaN/AlN MQWs were synthesized by MOCVD technique. It was demonstrated through PL spectroscopy under a near and above band edge excitation that the emission efficiency in MQWs:Er was enhanced by as much as nine times over GaN:Er epilayers with a comparable Er doped active layer thickness. The influences of the well and the barrier widths on the PL emission at 1.54 μm were studied. The results have shown that the optimal GaN/AlN MQWs:Er structures for achieving high 1.54 μm emission efficiencies are those with well width between 1.0 and 1.5 nm and the large possible barrier width below the critical thickness assuring lack of coupling of the quantum wells. The ability of tuning the carrier confinement in MQWs opens up the possibility of engineering Er doped III-nitride photonic devices with enhanced optical characteristics at 1.54 μm .

The materials growth effort was supported by JTO/ARO (W911NF-12-1-0330) and the optical characterization work was supported by NSF (ECCS-1200168). T. M. Al tahtamouni is grateful to the William J. Fulbright Commission of the United States and the Fulbright Committee in Jordan for the support of the Fulbright Visiting Scholarship at Texas Tech University. H. X. Jiang and J. Y. Lin are grateful to the AT&T Foundation for the support of Ed Whitacre and Linda Whitacre Endowed chairs.

¹M. Stachowicz, A. Kozanecki, C. G. Ma, M. G. Brik, J. Y. Lin, H. X. Jiang, and J. Zavada, *Opt. Mater.* **37**, 165 (2014).

²J. M. Zavada, S. X. Jin, N. Nepal, H. X. Jiang, J. Y. Lin, P. Chow, and B. Hertog, *Appl. Phys. Lett.* **84**, 1061 (2004).

³A. J. Steckl, J. Heikenfeld, M. Garter, R. Birkhahn, and D. S. Lee, *Compound Semiconductor* **6**, 48 (2000).

⁴M. Thaik, U. Hommerich, R. N. Schwartz, R. G. Wilson, and J. M. Zavada, *Appl. Phys. Lett.* **71**, 2641 (1997).

- ⁵R. G. Wilson, R. N. Schwartz, C. R. Abernathy, S. J. Pearton, N. Newman, M. Rubin, T. Fu, and J. M. Zavada, *Appl. Phys. Lett.* **65**, 992 (1994).
- ⁶J. T. Torvik, R. J. Feuerstein, J. I. Pankove, C. H. Qiu, and F. Namavar, *Appl. Phys. Lett.* **69**, 2098 (1996).
- ⁷H. Ennen, J. Schneider, G. Pomrenke, and A. Axmann, *Appl. Phys. Lett.* **43**, 943 (1983).
- ⁸M. R. Brown, A. F. J. Cox, W. A. Shand, and J. M. Williams, *Adv. Quantum Electron.* **2**, 69 (1974).
- ⁹J. M. Zavada and D. Zhang, *Solid-State Electron.* **38**, 1285 (1995).
- ¹⁰P. N. Favennec, H. L'Halidon, M. Salvi, D. Moutonnet, and Y. Le Guillou, *Electron. Lett.* **25**, 718 (1989).
- ¹¹R. Birkhahn, M. Garter, and A. J. Steckl, *Appl. Phys. Lett.* **74**, 2161 (1999).
- ¹²A. J. Neuhalfen and B. W. Wessels, *Appl. Phys. Lett.* **60**, 2657 (1992).
- ¹³R. Dahal, C. Ugolini, J. Y. Lin, H. X. Jiang, and J. M. Zavada, *Appl. Phys. Lett.* **93**, 033502 (2008); **97**, 141109 (2010).
- ¹⁴T. Arai, D. Timmerman, R. Wakamatsu, D. Lee, A. Koizumi, and Y. Fujiwara, *J. Lumin.* **158**, 70 (2015).
- ¹⁵I. W. Feng, J. Li, A. Sedhain, J. Y. Lin, H. X. Jiang, and J. Zavada, *Appl. Phys. Lett.* **96**, 031908 (2010).
- ¹⁶T. Ishiyama, S. Yoneyama, Y. Yamashita, Y. Kamiura, T. Date, T. Hasegawa, K. Inoue, and K. Okuno, *Physica B* **376**, 122 (2006).
- ¹⁷T. M. Al tahtamouni, J. Y. Lin, and H. X. Jiang, *J. Appl. Phys.* **113**, 123501 (2013).
- ¹⁸J. Nishio, L. Sugiura, H. Fujimoto, Y. Kokubun, and K. Itaya, *Appl. Phys. Lett.* **70**, 3431 (1997).
- ¹⁹K. C. Zeng, J. Z. Li, J. Li, J. Y. Lin, and H. X. Jiang, *Appl. Phys. Lett.* **76**, 3040 (2000).
- ²⁰C. S. Park, T. S. Kim, J. Y. Park, T. V. Cuong, H. W. Shim, E.-K. Suh, and C. H. Hong, *J. Korean Phys. Soc.* **43**(6), 1096 (2003).
- ²¹T. M. Al Tahtamouni, N. Nepal, J. Y. Lin, H. X. Jiang, and W. W. Chow, *Appl. Phys. Lett.* **89**, 131922 (2006).
- ²²H. Machhadani, M. Beeler, S. Sakr, E. Warde, Y. Kotsar, M. Tchernycheva, M. P. Chauvat, P. Ruterana, G. Nataf, Ph. De Mierry, E. Monroy, and F. H. Julien, *J. Appl. Phys.* **113**, 143109 (2013).
- ²³M. J. Paisley, Z. Sitar, J. B. Posthill, and R. F. Davis, *J. Vac. Sci. Technol., A* **7**(3), 701 (1989).
- ²⁴P. Ramvall, S. Tanaka, S. Nomura, P. Riblet, and Y. Aoyagi, *Appl. Phys. Lett.* **73**, 1104 (1998).